ISSN 1330-3651 (Print), ISSN 1848-6339 (Online) https://doi.org/10.17559/TV-20221122144345
Original scientific paper

Optimum Synthesis and Design of a Hood Linkage for Static Balancing in One-Step

Onur DENIZHAN*, Meng-Sang CHEW

Abstract: The conventional approach of the mechanism design process, generally, has a two-step procedure: Kinematic synthesis/analysis of the mechanism in the first step and optimization of the synthesized/analyzed mechanism based on optimization criteria in the second step. This study presents an approach that combines kinematic synthesis with the static balancing of the same, and optimization, into a one-step procedure. As an example of this one-step design process, a tension-spring assisted four-bar hood linkage optimal synthesis and design is performed in one-step. This one-step solution includes kinematic synthesis and analysis of the hood linkage, virtual work, static balancing with tension spring, and optimization in the presence of joint friction. The resulting design requires a minimum force to raise and lower the hood in the presence of unknown optimum levels of joint friction while the hood is statically balanced for its entire range of motion. A total of twelve different scenarios are investigated and the results are discussed.

Keywords: four-bar mechanism; kinematic analysis; kinematic synthesis; optimization; springs; static balancing

1 INTRODUCTION

This study presents an approach that combines kinematic synthesis with static balancing of same, into a one-step procedure. While the example used is an automotive hood linkage, the procedure presented is not limited to such an application. Suppose one is to design an automotive hood linkage system such that the hood is statically balanced through its entire range of motion, subjected to some dimensional constraints, with a requirement that a minimum force is applied to raise and close the hood. Joint friction in conjunction with a compensating tension spring is incorporated and designed to lower the hood opening and closing force.

The traditional approach, generally, is a two-step process. First, synthesize the hood linkage. Then, with the synthesized linkage, determine the attachment locations of the linear compensating spring, its stiffness, along with friction at the linkage joints, such that the objective of minimum hood lifting and closing forces is satisfied. This two-step procedure has been reported previously by Denizhan and Chew [1-4]. Note that the first step is a synthesis of a four-bar linkage, followed by a second step: Optimum static hood balancing. To do this in one single step, we need to combine four-bar linkage synthesis (Step 1) into the optimum static balancing process (Step 2) at the very outset of the problem formulation. This article presents a procedure of how such a one-step procedure is applied to designing a statically balanced automotive hood-linkage.

2 PRIOR WORK

The following are some of the many articles that have approached the design of a practical linkage problem by splitting the process into two or more steps: A given planar parallel-linked manipulator is optimized based on force balancing by Alici and Shirinzadeh [5]. The design procedure requires two steps: First, optimize the linkage mechanism, and second, a subsequent optimization for force balancing. The mechanism is synthesized before optimizing for the dynamic of the same by Rayner et al. [6]. An underactuated robotic finger is first designed and then applied optimization on the design by Sie and Gosselin [7]. A walking machine design process is introduced by Giesbrecy and it takes two steps: (i) synthesis of the machine and then (ii) optimization of the mechanism [8]. Such a sequential design approach is also taken by many others found in the literature: A reactionless parallel mechanism by Faoucault and Gosselin [9]; a spherical parallel mechanism by Chaker et al. [10]; a laparoscopic manipulator by Ma et al. [11]; an anthropomorphic finger by Demers and Gosselin [12]; a crank-rocker flapping-wing micro air-vehicle by McDonald and Agrawal [13]; a geared four-bar mechanism by Parlaktas et al. [14]; a planar manipulator by Mermertas [15]; a four-bar mechanism by Jaiswal and Jawale [16]. Spring-assisted mechanisms [20-35] are further examples of a long list of articles wherein the respective mechanisms are first designed/synthesized (Step 1) before optimization is performed (Step 2). The challenge is to reduce this design process to a single step: Both the mechanism synthesis and the optimization of the same, are performed together.

3 DESIGN OF AN AUTOMOTIVE HOOD LINKAGE

A very minimum of specifications is given in the design of a hood linkage. All these specifications are associated only with that of the automotive hood: (i) applied force locations at the opened- and closed-positions of the hood (plus other intermediate positions if so required), (ii) mass characteristics of the hood (c.g. location, and weight), and (iii) two acceptable regions for hinge locations on the hood. The objective is to achieve a minimum hood-lifting and lowering force that is assisted by friction at the joints, and a tension spring. The design challenge is to determine everything else below the hood and to perform this design in one-step. In other words, with just three design specifications for the automotive hood, the totality of this design problem is to simultaneously: (i) synthesize the dimensions of the four-bar linkage, (ii) determine the ground locations of the link pivots, (iii) locate the attachment points of a compensating spring and its stiffness characteristics, (iv) determine the optimal level of dry friction required at the joints of the four-bar to optimize the static balancing of the hood. A solution to this one-step design challenge is presented in this article.

In prior investigations, the four-bar hood linkage is first designed (Step 1) and a spring-loaded four-bar linkage mechanism is then optimized (Step 2) and in an additional step (Step 3), dry friction is subsequently applied to the linkage joints to minimize the forces needed to open and close the hood.

4 PROBLEM STATEMENT

The primary goal of this article is to show how to synthesize an optimum spring-loaded four-bar linkage mechanism for static balancing, in the presence of friction, in only one-step. This spring-loaded four-bar mechanism for an automotive engine hood serves only as a convenient example and the approach is not limited to this application not to the two precision positions for the hood linkage synthesis shown in this article.

Table 1 Constant design parameters

Constant Parameters	Values
l_h / m	1,2
W / N	12 kg × 9,8067 m/s^2 (117,68 N)
γ / rad	0,279 (16 degrees)
r / m	0,1

A tension spring-loaded four-bar linkage mechanism is shown in Fig. 1. The tension spring, all links, and joints are assumed massless, with a link [AC] being the driver link. The following hood specifications are given: Hood length (l_h) and hood weight (W) and fully-opened and fully-closed hood positions. All constant parameters for the hood are shown in Tab. 1.

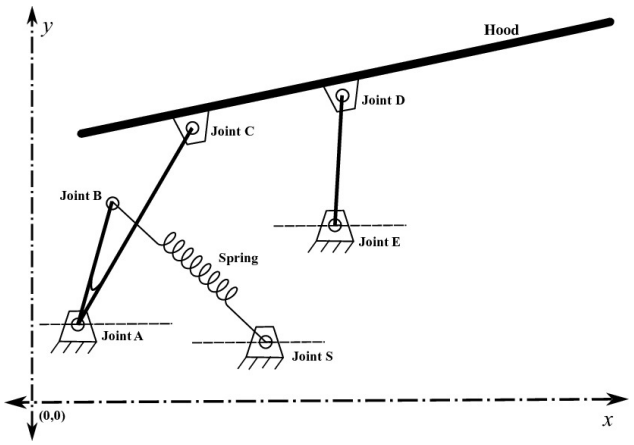

Figure 1 Four-bar linkage automotive hood with a tension spring

The layout of this article is as follows: In Section 1, we begin with a discussion of a two-position synthesis of the hood linkage. This provides the equations for synthesizing the four-bar hood linkage. Then, in Section 2, the virtual work equations are applied to the static balancing of the hood linkage. This equation provides the relationship between all the external forces acting on the linkage: The external force applied at the end of the hood, the weight of the hood, the friction in the linkage joints, as well as the energy stored in the tension spring. In Section 3, all the parameters to be determined that are presented in Sections 1 and 2, are then set up as design variables within an optimization procedure. This, briefly, is how the process of linkage synthesis and the static balancing design steps are integrated and optimized all together in a single step. In other words, the optimum parameters for the linkage synthesis and the static balancing are all optimized, not separately in two or more steps, but together within the same step. We now begin with a detailed description of each of the three sections below.

4.1 Two-Position Linkage Synthesis

A two-position kinematic synthesis with the right and left side dyads, vectors, and labels is shown in Fig. 2. The two-position kinematic synthesis of the same spring-loaded four-bar linkage mechanism can be found in standard textbooks such as in [17].

Referring to Fig. 2, dyads for the two links [AC] and [ED] are given below.

Left-side dyad:

$$we^{i\theta_0} = \frac{ze^{i(\psi+\alpha)} - p_{12}e^{i\delta} - ze^{i\psi}}{1-e^{i\theta_1}} \tag{1}$$

Right-side dyad:

$$ue^{i\phi_0} = \frac{se^{i(\sigma+\alpha)} - p_{12}e^{i\delta} - se^{i\sigma}}{1-e^{i\phi_1}} \tag{2}$$

where angle θ_0 is the angle of $\overrightarrow{W_1}$ (link [AC] at the first position ([AC$_1$])) and angle θ_1 is the angular difference between the first and last positions of link [AC] ([AC$_1$] and [AC$_2$] respectively). s is the length of the $\overrightarrow{S_1}$ and $\overrightarrow{S_2}$ ($|\overrightarrow{S_1}| = |\overrightarrow{S_2}|$, rigid link [DP]) and the angle σ is angle of $\overrightarrow{S_1}$ (link [D$_1$P$_1$], first position of [DP]) and the angle α is the angular difference between the first and last positions of link [DP] ([D$_1$P$_1$] and [D$_2$P$_2$] respectively), z is the length of the $\overrightarrow{Z_1}$ and $\overrightarrow{Z_2}$ ($|\overrightarrow{Z_1}| = |\overrightarrow{Z_2}|$, rigid link [CP]) and the angle ψ is the angle of $\overrightarrow{Z_1}$ (link [CP] first position ([C$_1$P$_1$])) and the angle α is angular difference between first and last positions of link [CP] ([C$_1$P$_1$] and [C$_2$P$_2$] respectively). u is the length of the $\overrightarrow{U_1}$ and $\overrightarrow{U_2}$ ($|\overrightarrow{U_1}| = |\overrightarrow{U_2}|$, rigid link [ED]) and angle ϕ_0 is the angle of $\overrightarrow{U_1}$ (link [ED] first position ([ED$_1$])) and the angle ϕ_1 is the angular difference between first and last positions of link [ED] ([ED$_1$] and [ED$_2$] respectively), p_{12} is the length of the $\overrightarrow{P_{12}}$ ($|\overrightarrow{R_1}|$) and the angle δ is the angle of $\overrightarrow{P_{12}}$.

In Eq. (1), there are eight variables and the two-position synthesis problem statement indicates that the parameters p_{12}, δ, and α are initially known because the first and last positions with the coupler link (which represents the automotive hood) and its rotation are specified [17]. Rewriting Eq. (1) into real and imaginary components, results in two equations with five variables, of which only two of the variables can be solved for. The other three can be treated as "free choices". In this study, parameters z, θ_1, and ψ are chosen as "free choices" and Eq. (1) can then be solved for w and θ_0.

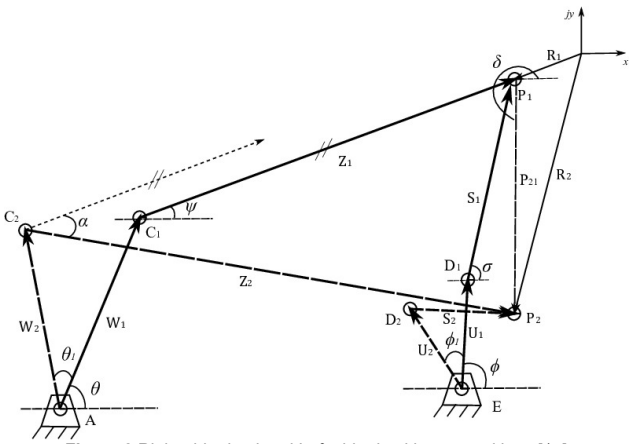

Figure 2 Right-side dyad and Left-side dyad in two positions [17]

Similarly, there are eight variables in Eq. (2), and values of p_{12}, δ, and α are known from the given two positions of the hood. The design variables s, σ, and ϕ_1 can be freely chosen so that Eq. (2) can then be solved for u and ϕ_0.

In a two-position synthesis of a four-bar linkage, a total of six "free choices" is available. These "free choices" now serve as design variables to optimize the entire linkage mechanism. If more precision positions are called for, the number of "free choices" and correspondingly, the design variables are reduced.

To simplify and conform to the equations in the rest of this article, angles θ and ϕ will be denoted as to the angular positions of the left and right links of the four-bar linkage, and they are equal to $(\theta_0 + \theta_1)$ and $(\phi_0 + \phi_1)$ respectively.

We will now look at deriving the static balancing force equation that provides the relationship among the many external forces acting on the hood linkage.

4.2 Virtual Work Formulation

The principle of virtual work states that the virtual work done by external active forces on an ideal mechanical system in equilibrium is zero for any and all virtual displacements consistent with the constraints. A model of a spring-loaded automotive hood linkage is shown in Fig. 3 with the angle γ between links [CP] and [CD] ($\angle$(PCD)) specified as 0,279 radian. This angle value is chosen arbitrarily and it is constant. Previously, the virtual work principle was introduced for the same spring-loaded automotive hood linkage mechanism and the following virtual work equation was presented for a static equilibrium condition of the mechanism [1-4]:

$$\delta W = P_{\mathrm{a}} \delta y_{\mathrm{p}} - \delta V_{\mathrm{s}} - \delta V_{\mathrm{h}} = 0 \tag{3}$$

where δW is the virtual work, δy_{p} is the virtual displacement of the point P, δV_{s} is the derivation of spring potential energy, δV_{h} is derivation of the potential energy of the hood and P_{a} is vertically applied force at the point P on the hood. From Eq. (3), the applied force P_{a} can be written as:

$$P_{\mathrm{a}} = \frac{\delta V_{\mathrm{s}} + \delta V_{\mathrm{h}}}{\delta y_{\mathrm{p}}} \tag{4}$$

Coulomb dry friction is assumed present in all four revolute joints (Joints A, C, D, and E) in this spring-loaded four-bar hood linkage. When the hood is opened and closed, coulomb friction in the joints creates a resistive force to hood motion. The virtual work equation as applied to the automotive hood linkage in the presence of an externally applied force, a compensating tension spring, hood weight, and joint friction can be shown to be [1-4]:

$$\delta W = P_{\mathrm{a}} \frac{\partial y_{\mathrm{p}}}{\partial \theta} - \frac{\partial V_{\mathrm{s}}}{\partial \theta} - \frac{\partial V_{\mathrm{h}}}{\partial \theta} \pm T_{\mathrm{A}} \mp T_{\mathrm{C}} \left(F_{\psi} - 1\right) \mp \pm T_{\mathrm{D}} \left(F_{\phi} - F_{\psi}\right) \pm T_{\mathrm{E}} F_{\phi} \tag{5}$$

where δW is the virtual work, P_{a} is the applied force, ∂y_{p} is the vertical virtual displacement of the force applied point on the hood (point P), ∂V_{s} and ∂V_{h} are conservative potentials of the tension spring and engine hood respectively. $T_{\mathrm{A}}, T_{\mathrm{C}}, T_{\mathrm{D}}$, and T_{E} are friction torques at joints A, C, D, and E respectively.

In the next section, we will look at bringing all the parameters presented in linkage synthesis, as well as the static balancing of the hood, under one umbrella wherein they are all optimized simultaneously through an optimization procedure.

4.3 Optimization - Problem Formulation

In this section, the goal of the optimization is to minimize the applied force (or balance force at peak points) to an automotive hood to open or close it. The optimization criterion has previously been investigated [2]. To minimize applied force to the hood, three objective function forms have been investigated, and the quartic $\int \left(P_a\right)^4 d\theta$ was found to be applicable and useful as an objective function. The result is the following multi-objective function which has been successfully used [2].

$$\min \; f = \eta_1 \int \left(P_{\mathrm{a_o}}\right)^4 \mathrm{d}\theta + \eta_2 \int \left(P_{\mathrm{a_c}}\right)^4 \mathrm{d}\theta \tag{6}$$

where η_1 and η_2 are weights of the functions in optimization multi-objective function. $P_{\mathrm{a_o}}$ and $P_{\mathrm{a_c}}$ are the applied vertical forces to open and close the engine hood respectively. Since the functions are quartic, they are always positive. The angle θ is the hood angle relative to the x - axis and $\eta_1 = \eta_2 = 1$ so that the opening and closing forces are weighted equally.

Six design variables are directly related to the tension spring: (i) tension spring constant (k); (ii) $\angle$BAC (β), (iii) & (iv) x_{s} and y_{s} coordinates of the spring attachment point S; (v) unloaded-spring length (l_0); and (vi) length of link [AB] (b).

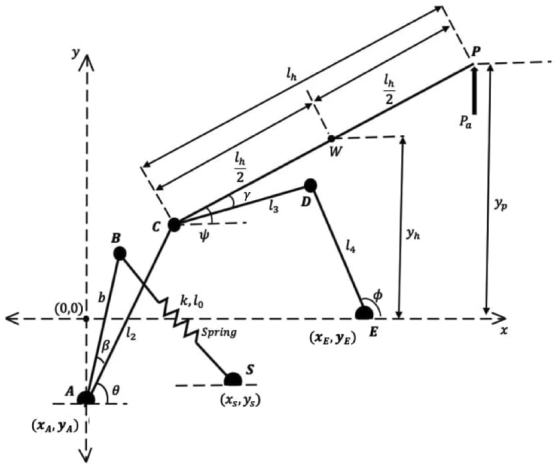

Figure 3 Four-bar hood linkage with a tension spring

These variables are illustrated in Fig. 3. Recall that from the two-position kinematic linkage synthesis formulation above, six "free choices" are available. In the optimization formulation, all six design variables for the tension spring plus four of the six "free choices" from the two-position synthesis formulation (θ_1, ψ, σ, and ϕ_1) can be set as design variables. Parameters *z* and *s* are the other two "free choices" in the two-position synthesis formulation and they are assigned as initially known parameters because the linkage position is based on given linkage and hood dimensions. Therefore, the parameter α in the two-position synthesis formulation can then be set as a design variable. The unknown joint friction provides yet another design variable resulting in optimization with a total of twelve design variables.

Two cases are investigated. These two cases are quite similar but have been included for completeness. Therefore, at this point, to expedite the study of this article, the reader is advised to just follow Case 1 and defer Case 2 to a subsequent reading. In Case 1, the tension spring-loaded four-bar linkage mechanism attachment points (Joints A and E) on the vehicle body are specified while in Case 2 the attachment points (Joints C and D) on the hood are specified. Each of these cases results in the following six optimization scenarios:

Scenario 1. (12 design variables): Six design variables from tension spring, there are five free choices in two-position kinematic synthesis plus joint friction torque can serve as design variables. Friction torque is assumed to equal in all four joints (Joints A, C, D, and E).

Scenario 2. (15 design variables): Friction torques are assumed as design variables in the four joints (Joints A, C, D, and E) and they are not equal. Three extra design variables are available compared to Scenario 1 above.

Scenario 3. (12 design variables): Friction is in Joint A only. Joints C, D, and E are frictionless.

Scenario 4. (12 design variables): Friction is in Joint C only. Joints A, D, and E are frictionless.

Scenario 5. (12 design variables): Friction is in Joint D only. Joints A, C, and E are frictionless.

Scenario 6. (12 design variables): Friction is in Joint E only. Joints A, C, and D are frictionless.

These six scenarios provide us a with greater understanding of the effects of friction in each as well as in all of the joints. Each of these six scenarios is investigated for both Cases 1 and 2.

In MATLAB Global Optimization Toolbox, fmincon - constrained nonlinear minimization was chosen as the solver because this problem is a constrained nonlinear optimization. Sequential Quadratic Programming (SQP) was also chosen to optimize the design because it is faster and uses less memory than the Active-Set algorithm [18].

4.3.1 Bounds on Variables

The bounds of the variables in the optimization problem are shown in Tab. 2. Based on the geometry and practical usage of the spring-loaded four-bar mechanism, boundary conditions for the design variables can be specified. For instance, *b* is the length between the spring attachment point on the link [AC] (point B) and Joint A in Fig. 3. The tension spring attachment point on the link [AC] cannot be on Joint A or very close to Joint A because the tension spring needs to have a motion based on its attachment point location to store or release potential energy during the motion of link [AC]. As a result, the lower bound of *b* is set as 0,2 m. Parameter *T* is the friction torque and in all six Scenarios, the boundary condition for friction torque is the same for all joints. For Scenarios wherein Joints A, C, D, and E can have different friction torques, parameters T_A, T_C, T_D, and T_E refer to the friction torques at Joints A, C, D, and E respectively. For friction torque and tension spring constant, the lower bounds are assumed as 0 Nm and 0,1 N/m respectively. In this article, the clockwise direction (CW) is assumed as the positive direction (positive sign) and the counter-clockwise direction (CCW) is assumed as the negative direction (negative sign) for friction torques.

Table 2 Optimization boundary conditions for the design variables

Design Variables	Lower Boundary	Upper Boundary
k / N/m	0,1	10^5
β / rad	–6,266	6,266
b / m	0,2	0,4
l_0 / m	0,001	0,1
x_s / m	0,5	0,6
y_s / m	–0,1	0,3
θ_1 / rad	0,3491	0,6981
α / rad	–1,309	–0,9599
ψ / rad	0,7854	1,1345
ϕ_1 / rad	0,4363	0,6109
σ / rad	0,7854	1,1345
T / Nm	0	10^5

4.3.2 Constraints on Design Variables

As shown in Tab. 2, it is possible for the unloaded-spring length (l_0) to be larger than the total spring length (l_s) during hood motion. To prevent such a case from happening an additional constraint is needed: $l_s > l_0$. This will ensure that the spring will always be in tension over the range of hood motion.

As previously mentioned, the two cases are investigated depending on whether the unknown joint locations of the links are on the engine hood (Case 1), or the car body (Case 2). For boundary conditions of these joints' attachment points, a round circular boundary is set to represent where each joint may be located. The radius of this circle boundary (*r*) is chosen at 0,1 m.

4.3.2.1 Case 1: Positions for Joints A and E on the Car Body are Specified

In Case 1, Joints A and E are specified and are fixed locations on the automobile body. On the other hand, attachment coordinates for Joints C (x_C, y_C) and D (x_D, y_D) on the engine hood are to be determined from the optimization process. Note that the unknown locations for Joints C and D are not prescribed as design variables such as angle θ or spring constant. It is actually from the optimization results for link length [AC] (w or l_2) or angle of link [AC] (θ) that allows us to back-calculate for the locations of Joints C and D after the optimization is completed. Configuration for Case 1 is shown in Fig. 4 for the hood at Position 1 (fully-open position).

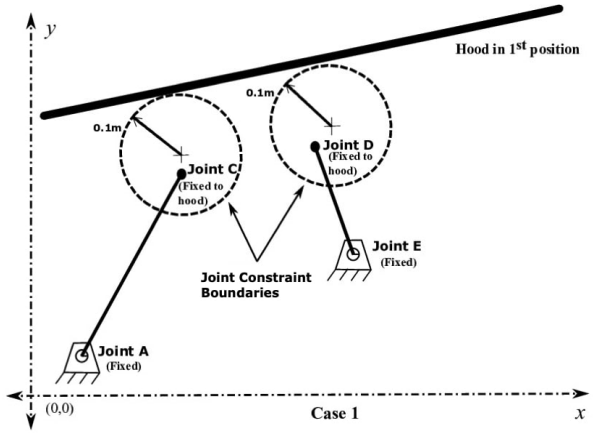

Figure 4 Case 1: Joints A and E are specified and are fixed on the car body

The general standard equation for a circle centered at (m, n) with radius r is given by $(x-m)^2+(y-n)^2=r^2$ by Stillwell [19]. Based on this, boundary conditions constraints for the coordinates of Joints C and D are respectively:

$$\left(x_C - x_{C_i}\right)^2 + \left(y_C - y_{C_i}\right)^2 < r^2 \tag{7}$$

and

$$\left(x_D - x_{D_i}\right)^2 + \left(y_D - y_{D_i}\right)^2 < r^2 \tag{8}$$

where (x_C, y_C), (x_D, y_D) are the respective centers of the circular bounds on the locations of Joints C and D. The coordinates (x_{C_i}, y_{C_i}) and (x_{D_i}, y_{D_i}) are actual coordinates of the Joints *C* and *D* that are constrained to be inside of the prescribed circular boundaries as set by the inequality constraints given by Eqs. (7) and (8) respectively.

4.3.2.2 Case 2: Positions for Joints C and D on the Hood Linkage are Specified

In Fig. 5, Joints C and D are specified locations fixed on the hood while the attachment point coordinates (x_A, y_A), (x_E, y_E) of Joints A and E respectively are assumed unknown but constrained to a circular bounded region on the car body. Similarly, as introduced in Case 1 above, the circular boundary constraints on Joints A and E can be shown respectively to be:

$$\left(x_A - x_{A_i}\right)^2 + \left(y_A - y_{A_i}\right)^2 < r^2 \tag{9}$$

and

$$\left(x_E - x_{E_i}\right)^2 + \left(y_E - y_{E_i}\right)^2 < r^2 \tag{10}$$

where (x_A, y_A), (x_E, y_E) are the respective centers of the circular bounds on the locations of Joints A and E. The coordinates (x_{A_i}, y_{A_i}) and (x_{E_i}, y_{E_i}) are actual coordinates of the Joints A and E that are constrained to be inside of the prescribed circular boundaries as set by the inequality constraints given by Eqs. (9) and (10) respectively.

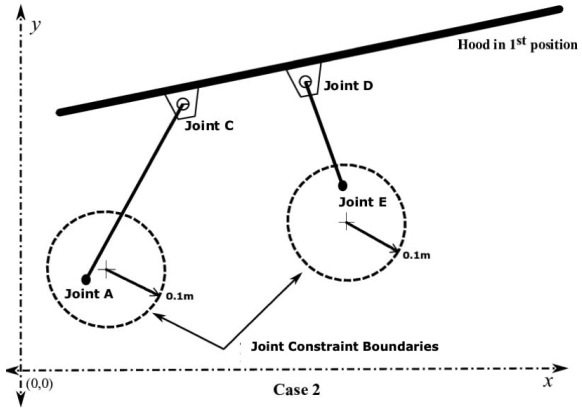

Figure 5 Case 2: Joints C and D are specified and are fixed on the engine hood

The optimization setup of the multi-objective problem with constraints (including Case 1 and Case 2 boundary constraints) is summarized in Tab. 3 below.

Table 3 Summary of the optimization setup for Cases 1 and 2 with constraints on the tension spring and the locations of the respective joints

Case 1	
minimize	$f=\eta_1\int\left(P_{a_o}\right)^4 \mathrm{d}\theta+\eta_2\int\left(P_{a_c}\right)^4 \mathrm{d}\theta$
subject to	$l_s > l_0$ $\left(x_C - x_{C_i}\right)^2 + \left(y_C - y_{C_i}\right)^2 < r^2$ $\left(x_D - x_{D_i}\right)^2 + \left(y_D - y_{D_i}\right)^2 < r^2$
Case 2	
minimize	$f=\eta_1\int\left(P_{a_o}\right)^4 \mathrm{d}\theta+\eta_2\int\left(P_{a_c}\right)^4 \mathrm{d}\theta$
subject to	$l_s > l_0$ $\left(x_A - x_{A_i}\right)^2 + \left(y_A - y_{A_i}\right)^2 < r^2$ $\left(x_E - x_{E_i}\right)^2 + \left(y_E - y_{E_i}\right)^2 < r^2$

5 RESULTS

A total of twelve scenarios are investigated, six for each of the two cases. In Case 1, the tension spring-loaded

four-bar linkage mechanism attachment points (Joints A and E) on the vehicle body are specified while for Case 2, the attachment points (Joints C and D) on the hood are specified. Tab. 4 summarizes the optimization results for Case 1 and Case 2.

From Tab. 4, it can be seen that the tension spring stiffness for Case 2 is lower than that for Case 1, except where in Scenario 6, there is only a 20 N/m difference between the two cases. Also, note that optimum friction torques in Case 2 are also lower than those in Case 1. However, in Scenario 6, the optimum friction torques are the same for both cases. There is also not much difference between other design variables' optimization results for both cases. Tab. 4 also shows that the lowest joint friction torque happens when the friction in all four joints (Joints A, C, D and E) is equal in Scenario 1. In Scenario 2, the optimum friction torque is only required in Joint A with zero friction required at the other joints. A comparison of Cases 1 and 2 in Tab. 4 shows that the lowest friction torque happens in Scenario 4 and the highest friction happens in Scenario 3.

Table 4 Cases 1 and 2 Optimization results for the various scenarios

Design Variables	CASES 1 & 2 Optimization Results											
	Scenario 1		Scenario 2		Scenario 3		Scenario 4		Scenario 5		Scenario 6	
	Case 1	Case 2	Case 1	Case 2	Case 1	Case 2	Case 1	Case 2	Case 1	Case 2	Case 1	Case 2
k / N/m	2092,24	1971,02	2078,39	1193,74	2078,39	1193,74	2727,82	700,15	2002,28	1390,63	1861,37	1881,86
β / rad	–6,266		–6,266	–6,257	–6,266	–6,257	–0,585	–6,241	–6,266	5,515	–6,266	
b / m	0,202	0,207	0,202	0,229	0,202	0,229	0,205	0,222	0,206	0,235	0,227	0,23
l_0 / m	0,1		0,1		0,1		0,1	0,097	0,1	0,071	0,1	
x_s / m	0,5		0,5	0,501	0,5	0,501	0,568	0,507	0,5	0,577	0,5	
y_s / m	0,3		0,3		0,3		0,248	0,293	0,3	0,091	0,3	
θ_1 / rad	0,698	0,694	0,698	0.681	0,698	0,681	0,698	0,694	0,698	0,675	0,698	
α / rad	–1,203		–1,203	–1.241	–1,203	–1,241	–1,2	–1,253	–1,203	–1,22	–1,203	–1,204
ψ / rad	1,003	1,001	1,002	1.024	1,002	1,024	1,036	1,024	1,003	1,029	1,002	1,003
ϕ_1 / rad	0,486	0,436	0,486	0.434	0,486	0,434	0,436	0,438	0,436	0,446	0,436	
σ / rad	0,987	0,974	0,986	1.008	0,986	1,008	0,98	0,999	0,988	1,001	0,986	
T / Nm	0,752	0,75	Not investigated		Not investigated		Not investigated		Not investigated		Not investigated	
T_A / Nm	Not investigated		5,121	2,807	5,121	2,807	Not investigated		Not investigated		Not investigated	
T_C / Nm	Not investigated		0		Not investigated		1,654	1,101	Not investigated		Not investigated	
T_D / Nm	Not investigated		0		Not investigated		Not investigated		2,584	1,403	Not investigated	
T_E / Nm	Not investigated		0		Not investigated		Not investigated		Not investigated		2,409	2,4

6 DISCUSSION

From Tab. 4, both cases show that the optimum joint friction is lowest when it is constrained to be equal for all joints (Scenario 1). In other words, the magnitude of the required friction torque is lowest when every joint is set to carry the same friction torque. On the other hand, when the optimization has the freedom to assign any friction torque at all four joints (Scenario 2), the lowest (optimum) occurs when friction torque is specified only at Joint A. In other words, the optimum is to have friction only at Joint A and frictionless in the other three joints. Scenario 3 also confirms this observation.

Scenarios 3 through 6 constraint the optimization to allocate friction torque only at Joints A, C, D, or E, respectively. A comparison of these four scenarios shows that the required optimum joint friction is when that joint is the only joint to be allocated friction torque.

Previously, sensitivity analysis of design parameters is investigated for the same mechanism to understand how the mechanism is sensitive to design parameters by Denizhan and Chew [1]. However, joint friction is ignored in this study; hence, another sensitivity analysis can be investigated for an understanding of the mechanism sensitivity to design variables in the presence of joint friction.

As mentioned before, the one-step solution approach is not just valid for two precision positions for the hood linkage synthesis. For instance, in the current two-position kinematic synthesis formulation, there are six "free choice" parameters, which will then serve as design variables in the optimization procedure. However, if a three-position kinematic synthesis formulization is required, there will be a total of only four "free choice" parameters in left- and right-side dyads [17], a reduction of two "free choices". All other virtual work and optimization formulizations in this one-step design approach will remain the same. In other words, increasing the number of precision positions will only reduce number of design variables for the optimizer. This is because precision position specifications act as constraints on the total design space, thereby reducing the design freedom given to the optimizer. A comparison of the results from the specification of different number of precision positions will be a subject for further study.

This article is primarily a theoretical investigation to demonstrate the practicality of a design procedure that designs a mechanical system optimally in just one single step, given a very minimum of specifications. Experimental verification of these results from this article will be a subject of a future investigation.

7 CONCLUSIONS

In this article, a four-bar linkage compensated by a tension spring is designed for static balancing in the presence of joint friction to assist in the same. The procedure is accomplished in one step using an optimization procedure. What this means is that the optimization parameters for the linkage synthesis and those for static balancing of the hood linkage, are all optimized together within the same optimization procedure. Although in this article a two-precision position linkage synthesis is

used, this approach is also valid for more than two positions. Friction at the joints of the linkage is also optimally determined as part of the optimization, to assist in minimizing the applied force for opening and closing the hood. Optimal locations of the joints on the hood or the car body (two different design cases) are also automatically determined along with the attachment points of the tension spring and its physical parameters.

Acknowledgements

The authors wish to acknowledge that the basic tenets of this research idea came from Professor Ferdinand Freudenstein of Columbia University over four decades ago. The authors also wish to express their gratitude to the Ministry of National Education of the Republic of Turkey which indirectly made this work possible.

8 REFERENCES

[1] Denizhan, O. & Chew, MS. (2018). Linkage mechanism optimization and sensitivity analysis of an automotive engine hood. *International Journal of Automotive Science and Technology*, *2*, 7-16. https://doi.org/10.30939/ijastech..364438

[2] Denizhan, O. & Chew, MS. (2019). Optimum design of a spring-loaded linkage mechanism in the presence of friction for static balancing. *Journal of Engineering Design and Analysis*, *2*(1), 1-7. https://doi.org/10.24321/2582.5607.201901

[3] Denizhan, O. (2015). *Three-Position Four-Bar Linkage Mechanism Synthesis, Static Balancing and Optimization of Automotive Engine Hood*. Master's Thesis, Lehigh University.

[4] Denizhan, O. (2021). *Incorporation of Kinematic Analysis, Synthesis and Optimization into Static Balancing*. Doctoral dissertation, Lehigh University.

[5] Alıcı, G. & Shirinzadeh, B. (2004). Optimum synthesis of planar parallel manipulators based on kinematic isotropy and force balancing. *Robotica*, *22*(1), 97-108. https://doi.org/10.1017/S0263574703005216

[6] Rayner, R. M. C., Sahinkaya, M. N., & Hicks, B. (2017). Improving the design of high-speed mechanisms through multi-level kinematic synthesis, dynamic optimization and velocity profiling. *Mechanism and Machine Theory*, *118*, 100-114. https://doi.org/10.1016/j.mechmachtheory.2017.07.022

[7] Sie, L.M. & Gosselin, C. M. (2002, October). Dynamic simulation and optimization of underactuated robotic fingers. *Proceedings of the ASME 2002 International Design Engineering Technical Conferences and Computers and Information in Engineering Conference*, *5*, 191-199. https://doi.org/10.1115/DETC2002/MECH-34220

[8] Giesbrecht, D. (2010). *Design and Optimization of a One-Degree-Of- Freedom Eight-Bar Leg Mechanism for a Walking Machine*. Master's Thesis, The University of Manitoba.

[9] Foucault, S. & Gosselin, C. M. (2004). Synthesis, design, and prototyping of a planar three degree-of-freedom reactionless parallel mechanism. *Journal of Mechanical Design*, *126*(6), 992-999. https://doi.org/10.1115/1.1798211

[10] Chaker, A., Laribi, M. A., Zeghloul, S. et al. (2011, November). Design and optimization of spherical parallel manipulator as a haptic medical device. *IECON 2011 - 37th Annual Conference of the IEEE Industrial Electronics Society*, 80-85. https://doi.org/10.1109/IECON.2011.6119292

[11] Ma, R., Wang, W., Du, Z. et al. (2012, May). Design and optimization of manipulator for laparoscopic minimally invasive surgical robotic system. *2012 IEEE International Conference on Mechatronics and Automation*, 598-603. https://doi.org/10.1109/ICMA.2012.6283175

[12] Demers, L. A. & Gosselin, C. (2009, May). Kinematic design of an ejection-free underactuated anthropomorphic finger. *2009 IEEE International Conference on Robotics and Automation*, 2086-2091. https://doi.org/10.1109/ROBOT.2009.5152301

[13] McDonald, M. & Agrawal, S. K. (2010). Design of a bio-inspired spherical four-bar mechanism for flapping-wing micro air-vehicle applications. *Journal of Mechanisms and Robotics*, *2*(2), 021012. https://doi.org/10.1115/1.4001460

[14] Parlaktas, V., Soylemez, E., & Tanık, E. (2010). On the synthesis of a geared four-bar mechanism. *Mechanism and Machine Theory*, *45*(8), 1142-1152. https://doi.org/10.1016/j.mechmachtheory.2010.03.007

[15] Mermertas, V. (2004). Optimal design of manipulator with four-bar mechanism. *Mechanism and Machine Theory*, *39*(5), 545-554. https://doi.org/10.1016/j.mechmachtheory.2003.12.002

[16] Jaiswal, A. & Jawale, H. P. (2018). Synthesis and optimization of four bar mechanism with six design parameters. *AIP Conference Proceedings 1943*, *020014*. https://doi.org/10.1063/1.5029590

[17] Norton, R. L. (2020). *Design of Machinery: An Introduction to the Synthesis and Analysis of Mechanisms and Machines*. 6th ed.: McGraw-Hill.

[18] Venkataraman, P. (2009). *Applied Optimization with MATLAB Programming*. 2nd ed.: Wiley.

[19] Stillwell, J. (2005). *The Four Pillars of Geometry*. 1st ed.: Springer.

[20] Brinkman, M. L. & Herder, J. L. (2002, October). Optimizing balanced spring mechanism. *Proceedings of the ASME 2002 International Design Engineering Technical Conferences and Computers and Information in Engineering Conference*, *5*, 737-745. https://doi.org/10.1115/DETC2002/MECH-34284

[21] Drenth, J. & Herder, J. L. (2004, October). Numerical optimization of the design of a laparoscopic grasper, statically balanced with normal springs. *Proceedings of the ASME 2004 International Design Engineering Technical Conferences and Computers and Information in Engineering Conference*, *2*, 923-933. https://doi.org/10.1115/DETC2004-57373

[22] teRiele, F. L. S. & Herder, J. L. (2001, September). Perfect static balance with normal springs. *Proceedings of the ASME 2001 International Design Engineering Technical Conferences and Computers and Information in Engineering Conference*, *2A*, 571-578. https://doi.org/10.1115/DETC2001/DAC-21069

[23] Herder, J. L. (2001). *Energy-Free Systems: Theory, Conception and Design of Statically Balanced Spring Mechanisms*. Doctoral dissertation, Deft University of Technology.

[24] van Dorsser, W. D., Barrents, R., Wisse, B. M. et.al. (2008). Energy-free adjustment of gravity equilibrators by adjusting the spring stiffness. *Proceedings of the Institution of Mechanical Engineers, Part C: Journal of Mechanical Engineering Science*, *222*(9), 1839-1846. https://doi.org/10.1243/09544062JMES832

[25] French, M. J. & Widden, M. B. (2000). The spring-and-lever balancing mechanism, George Carwardine and the anglepoise lamp. *Proceedings of the Institution of Mechanical Engineers, Part C: Journal of Mechanical Engineering Science*, *214*(3), 501-508. https://doi.org/10.1243/0954406001523137

[26] Takahashi, T., Zehnder, J., Okuno, H. G. et. al. (2019). Computational design of statically balanced planar spring mechanism. *IEEE Robotics and Automation Letters*, *4*(4), 4438-4444. https://doi.org/10.1109/LRA.2019.2929984

[27] teRiele, F. L. S., Herder, J. L., & Hekman, E. E. G. (2004, September). Spatial static gravity balancing with ideal springs. *Proceedings of the ASME 2004 International*

Design Engineering Technical Conferences and Computers and Information in Engineering Conference, *2*, 425-432. https://doi.org/10.1115/DETC2004-57166

[28] Herder, J. L. (1998). Design of spring force compensation systems. *Mechanism and Machine Theory*, *33*(1-2), 151-161. https://doi.org/10.1016/S0094-114X(97)00027-X

[29] Yang, Z. W. & Lan, C. C. (2015). An adjustable gravity-balancing mechanism using planar extension and compression springs. *Mechanism and Machine Theory*, *92*, 314-329. https://doi.org/10.1016/j.mechmachtheory.2015.05.006

[30] Delissen, A. T. M. A., Radaelli, G., & Herder, J. L. (2017). Design and optimization of a general planar zero free length spring. *Mechanism and Machine Theory*, *117*, 56-77. https://doi.org/10.1016/j.mechmachtheory.2017.07.002

[31] Woo, J., Seo, J. T., & Yi, B. J. (2019). A static balancing method for variable payloads by combination of a counterweight and spring and its application as a surgical platform. *Applied Sciences*, *9*(19), 3955. https://doi.org/10.3390/app9193955

[32] Perreault, S., Cardou, P., & Gosselin, C. (2014). Approximate static balancing of a planar parallel cable-driven mechanism based on four-bar linkages and springs. *Mechanism and Machine Theory*, *79*, 65-79. https://doi.org/10.1016/j.mechmachtheory.2014.04.008

[33] Lin, P. Y., Shieh, W. B., & Chen, D. Z. (2013). A theoretical study of weight-balanced mechanisms for design of spring assistive mobile arm support (MAS). *Mechanism and Machine Theory*, *61*, 156-167. https://doi.org/10.1016/j.mechmachtheory.2012.11.003

[34] Shin, E. & Streit, D. A. (1991). Spring equilibrator theory for static balancing of planar pantograph linkages. *Mechanism and Machine Theory*, *26*(7), 645-657. https://doi.org/10.1016/0094-114X(91)90027-2

[35] Streit, D. A. & Gilmore, B. J. (1989). Perfect spring equilibrators for rotatable bodies. *ASME Journal of Mechanisms, Transmissions, and Automation in Design*, *111*(4), 451-458. https://doi.org/10.1115/1.3259020

Contact information:

Onur DENIZHAN, PhD, Lecturer
(Corresponding author)
Batman University,
Kültür, Türkiye Petrolleri A. O. Blv.,
Merkez, Batman 72060. Turkey
E-mail: onur.denizhan@batman.edu.tr

Meng-Sang CHEW, PhD, Associate Professor
Lehigh University,
Packard Lab 256B,
19 Memorial Dr. West,
Bethlehem, PA 18015. USA
E-mail: mc0p@lehigh.edu